

X-ray study on the evolution of thermal motion in the ferroelectric phase of  $\text{NaNO}_2$ 

T. Gohda and M. Ichikawa

Division of Physics, Graduate School of Science, Hokkaido University, Sapporo 060-0810, Japan

T. Gustafsson and I. Olovsson

Inorganic Chemistry, Ångström Laboratory, Uppsala University, Box 538, S751-21, Uppsala, Sweden

(Received 29 May 2000; published 11 December 2000)

The crystal structure of  $\text{NaNO}_2$  has been refined in the ferroelectric phase at 338, 378, and 418 K. The evolution of the thermal motion with increasing temperature has been studied by comparing the anisotropic displacement parameters, including earlier values at low temperatures. The results support the rotation of  $\text{NO}_2$  around the  $c$  axis as the mechanism of polarization reversal. It is strongly suggested that the coupling between the translational motion along the  $b$  axis and the rotational motion of the  $\text{NO}_2$  ion becomes stronger approaching to  $T_c$ , reducing the effective potential barrier for  $\text{NO}_2$  rotation. The location of the rotation center is estimated to be slightly closer to the N atom. The electron density contribution from a small amount of disordered atoms has been found.

DOI: 10.1103/PhysRevB.63.014101

PACS number(s): 61.10.Eq, 77.84.Bw

## I. INTRODUCTION

Sodium nitrite,  $\text{NaNO}_2$ , is one of the typical ferroelectrics with the simplest crystal structure. A schematic illustration of the structure is shown in Fig. 1. In the ferroelectric phase, which is stable below about 436 K (orthorhombic,  $Im2m$ ,  $Z=2$ ), the structure is expected to have only the solid circle arrangement in Fig. 1 at 0 K, but with increasing temperature the polarization-reversed broken circle arrangement becomes successively larger. The structure undergoes a transition to a paraelectric phase at around 437 K, and the ratio between the solid and broken circle orientations becomes 1:1. Between the ferroelectric and paraelectric phase there is a sinusoidal incommensurate phase at around 436 K, which is stable only in a very narrow temperature range, of the order of 1 K.

The phase transition of  $\text{NaNO}_2$  is classified as a typical order-disorder type, where the transition is driven by order-

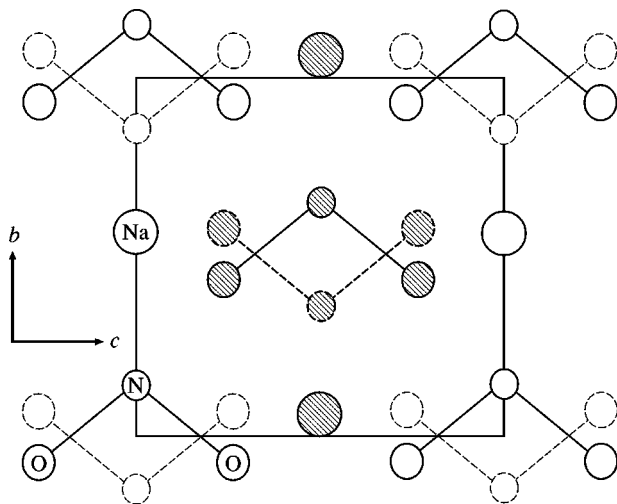


FIG. 1. Crystal structure of  $\text{NaNO}_2$  in the ferroelectric phase projected along the  $a$  axis. The shaded atoms are at  $x = \pm \frac{1}{2}$ . The solid circle arrangement (majority part); the broken circle arrangement (minority part).

ing of the  $\text{NO}_2$  ions and is described by an Ising model.<sup>1</sup> The first fundamental question concerning the phase transition is the mechanism of the polarization reversal. Three basic types of polarization reversal models have been proposed, as shown in Fig. 2; (1) rotation of  $\text{NO}_2$  around the  $c$  axis, (2) rotation of  $\text{NO}_2$  around the  $a$  axis, and (3) tunneling of the N atom through the potential barrier between two oxygen atoms.<sup>2</sup> Since then many investigations have been devoted to reveal the mechanism of the  $\text{NO}_2$  polarization reversal. The majority of the earlier results support the  $c$ -axis rotation model, i.e., all structure analyses by neutron<sup>3,4</sup> and x-ray<sup>5-7</sup> diffraction, x-ray topography,<sup>8</sup> neutron time-of-flight,<sup>9</sup> time-resolved x-ray diffraction,<sup>10</sup>  $^{23}\text{Na}$  nuclear magnetic resonance,<sup>11</sup>  $^{14}\text{N}$  nuclear quadrupole resonance,<sup>12</sup> dc resistivity, differential thermal analysis and lattice constants,<sup>13</sup> microscopic model calculation,<sup>14</sup> molecular-dynamics<sup>15,16</sup> and *ab initio* calculations.<sup>17</sup> Some studies, however, support the  $a$ -axis rotation model; i.e., infrared<sup>2,18</sup> and Raman<sup>19,20</sup> spectroscopy. The second fundamental question is the dynamics of the polarization reversal. Although an Ising model can be used formally to describe the solid and broken positions of  $\text{NO}_2$  in Fig. 1 (as the position *before* and *after* the reversal), it does not give much insight into the dynamics on a microscopic level. If we, for example, compare  $\text{NaNO}_2$  with  $\text{KH}_2\text{PO}_4$ ,<sup>1</sup> both compounds of order-disorder type, a distinct difference is recognized; the steric barrier is expected to be much higher in the former case during reversal of the direction of polarization ( $180^\circ$  rotation of an asymmetric planar

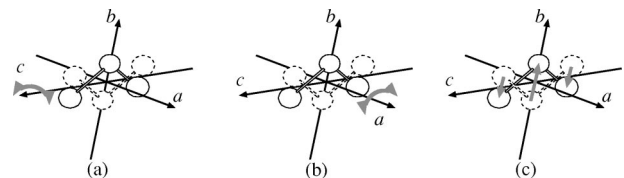


FIG. 2.  $\text{NO}_2$  reversal models. (a) Rotation about the  $c$  axis, (b) rotation about the  $a$  axis, and (c) penetration of N through the oxygen atoms.

TABLE I. Data collection.  $N_{\text{obs}}$  is number of reflections observed and  $N_{\text{ref}}$  is number of reflections used in refinement.

	338 K	378 K	418 K
	Mo $K\alpha$	$\lambda = 0.71073 \text{ \AA}$	
$2\theta_{\text{max}} (\circ)$	99	100	90
$h$	$-7 \leq h \leq 6$	$-7 \leq h \leq 6$	$-7 \leq h \leq 6$
$k$	$-11 \leq k \leq 5$	$-12 \leq k \leq 5$	$-11 \leq k \leq 5$
$l$	$-11 \leq l \leq 9$	$-11 \leq l \leq 9$	$-10 \leq l \leq 9$
$N_{\text{obs}}$	1828	1885	1994
$N_{\text{ref}}$	1017	1061	934

molecule in the case of  $\text{NO}_2$ ). The polarization reversal is therefore possibly assisted by coupling of the lattice vibration modes. From a structural point of view, a study of the evolution of the thermal motion with temperature may give important information. Although some structural studies have been done in the temperature range between room temperature and the transition temperature  $T_c$  in the ferroelectric phase,<sup>5,6,21</sup> data in a wider temperature range and of better precision would be preferable when investigating the dynamics of the polarization reversal.

Recently we studied the structure at room temperature<sup>24</sup> and at 30 K.<sup>22</sup> New data at 338, 378, and 418 K have now been collected. These studies together with that at 120 K by Okuda *et al.*<sup>23</sup> give an opportunity to investigate the dynamics of the polarization reversal based on data in a wide tem-

TABLE II. Cell parameters.

	338 K	378 K	418 K
	Mo $K\alpha_1$	$\lambda = 0.70930 \text{ \AA}$	
$a (\text{\AA})$	3.5817(7)	3.6029(7)	3.6303(15)
$b (\text{\AA})$	5.5873(5)	5.6037(5)	5.6331(12)
$c (\text{\AA})$	5.3869(7)	5.3851(6)	5.3776(13)
$V_c (\text{\AA}^3)$	107.801(15)	108.723(15)	109.97(3)

perature range. From the new data, in particular at 418 K, which is close to  $T_c$ , evidence for the existence of a small fraction of disordered  $\text{NO}_2$  could also be detected; no one has so far observed such disorder.

In this paper, we aim to (1) investigate the dynamics of the polarization reversal of  $\text{NO}_2$  (such as the coupling of rotational and translational modes and the location of the rotation axis), and to get additional information about the mechanism of the polarization reversal and (2) find evidence for the existence of small amount of disordered  $\text{NO}_2$ .

## II. EXPERIMENT

Single crystals of  $\text{NaNO}_2$  were grown from an aqueous solution around room temperature. A prismatic crystal of dimensions  $0.05 \times 0.08 \times 0.19 \text{ mm}$  with well-developed natural faces was used as specimen. X-ray intensity measurements were made using Mo  $K\alpha$  radiation ( $\lambda = 0.71073 \text{ \AA}$ )

TABLE III. Refined parameters and discrepancy factors. Displacement factor is defined by  $T = \exp\{-2\pi^2(h^2a^2U_{11} + \dots + 2hka^*b^*U_{12} + \dots)\}$ .  $f$  is occupancy factor,  $R = \Sigma|F_o^2 - F_c^2|/\Sigma F_o^2$ ,  $wR = \{\Sigma \sigma^{-2}(F_o^2 - F_c^2)^2/\Sigma \sigma^{-2}F_o^4\}^{1/2}$ , respectively.

		338 K	378 K	418 K
Na	$x$	0	0	0
	$y$	0.5422(1)	0.5414(1)	0.5393(1)
	$z$	0	0	0
N	$x$	0	0	0
	$y$	0.0760(2)	0.0751(2)	0.0735(2)
	$z$	0	0	0
O	$x$	0	0	0
	$y$	-0.0443(1)	-0.0444(1)	-0.0447(1)
	$z$	0.1947(1)	0.1943(1)	0.1940(1)
Na	$U_{11}$	0.0327(2)	0.0382(2)	0.0444(3)
	$U_{22}$	0.0254(2)	0.0299(2)	0.0374(3)
	$U_{33}$	0.0247(2)	0.0290(2)	0.0344(2)
N	$U_{11}$	0.0357(3)	0.0430(3)	0.0530(5)
	$U_{22}$	0.0237(4)	0.0292(4)	0.0377(6)
	$U_{33}$	0.0237(3)	0.0276(3)	0.0338(4)
O	$U_{11}$	0.0453(3)	0.0535(3)	0.0639(4)
	$U_{22}$	0.0328(3)	0.0391(3)	0.0481(5)
	$U_{33}$	0.0216(2)	0.0257(2)	0.0314(2)
	$U_{23}$	0.0036(2)	0.0042(2)	0.0053(2)
	$f$	0.992	0.972	0.916
	$R(F^2)$	0.0491	0.0528	0.0538
	$wR(F^2)$	0.0564	0.0579	0.0679

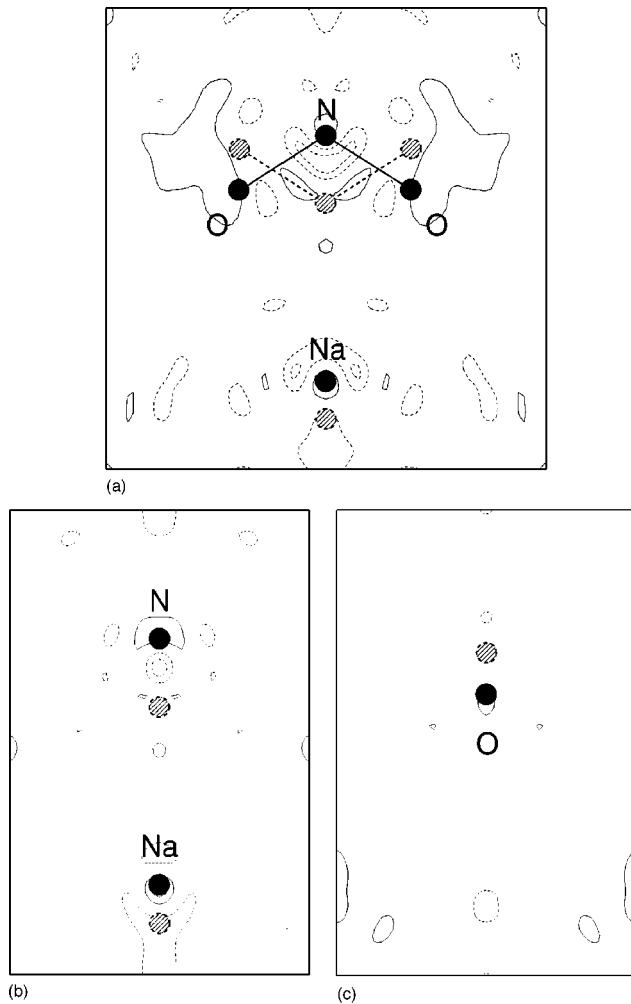


FIG. 3. Residual maps for the disordered model at 418 K (contribution from both of the major and the minor part was subtracted), (a)  $b$ - $c$  plane ( $x=1/2$ ), (b)  $a$ - $b$  plane ( $z=1/2$ ), and (c)  $a$ - $b$  plane (passing through O), respectively. Contour intervals at  $0.1 e \text{ \AA}^{-3}$ .

by an  $\omega$ - $2\theta$  scanning mode at Uppsala University. A microfurnace<sup>25</sup> was attached to the goniometer head of a Stoe four-circle diffractometer. The intensities were corrected for time variation of the standard reflections.<sup>26</sup> Absorption correction, based on the size and shape of the specimen, was made by numerical integration with linear absorption coefficient  $\mu = 3.717 \text{ cm}^{-1}$  (338 K),  $3.686 \text{ cm}^{-1}$  (378 K), and  $3.644 \text{ cm}^{-1}$  (418 K). The calculated transmission factor  $A$  was  $0.9373 < A < 0.9605$  (338 K),  $0.9378 < A < 0.9608$  (378 K), and  $0.9385 < A < 0.9596$  (418 K). Experimental details of the data collection are listed in Table I, and cell parameters in Table II. All crystallographic calculations including analyses were made using the program system by Lundgren.<sup>27</sup>

### III. ANALYSES AND RESULTS

The structure for each data set was determined by least-squares refinement with the program DUPALS.<sup>27</sup> The quantity minimized was  $\chi^2 = \sum (F_o^2 - F_c^2)^2 / \sigma^2(F_o^2)$ , where  $F_o$  and  $F_c$  denote the amplitude of the observed and calculated structure

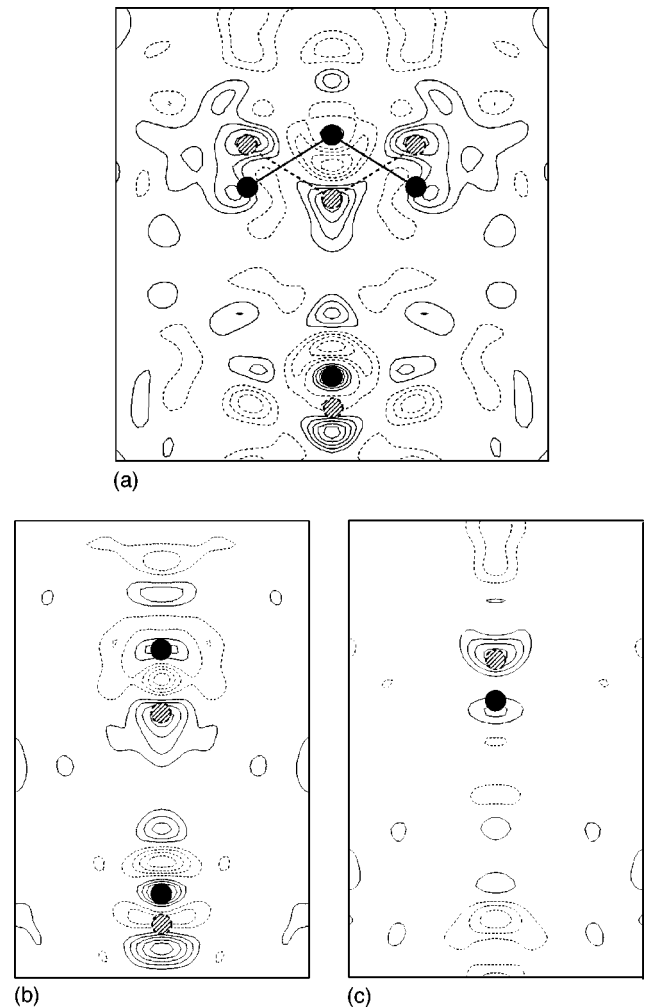


FIG. 4. Residual maps for the ordered model at 418 K (contribution only from the major part was considered and subtracted), (a)  $b$ - $c$  plane ( $x=1/2$ ), (b)  $a$ - $b$  plane ( $z=1/2$ ), and (c)  $a$ - $b$  plane (passing through O), respectively. Contour intervals at  $0.1 e \text{ \AA}^{-3}$  (cf. Fig. 3 as for atom label).

factors, respectively, and  $\sigma(F_o^2)$  is the standard deviation of  $F_o^2$  including instrumental instability. All reflections were used in the refinement without averaging, although the unique reflections were only one octant of the whole reciprocal space (some reflections, which had been measured repeatedly, were averaged).

All atoms were assumed to be spherical and neutral. Atomic scattering factors and anomalous scattering factors were taken from *International Tables for Crystallography*, Volume C, 1992. Isotropic secondary-extinction correction with Lorentzian distribution according to Becker and Coppens formalism<sup>28</sup> was applied.

As  $\text{NaNO}_2$  is ferroelectric (with an order parameter less than one) in the temperature region of the present paper, observed structure factors may include some contribution from a small fraction of disordered molecules. The amount of contribution is expected to correspond to the order parameter (most notably at 418 K). Therefore the occupancy factor  $f$ , which represents the ratio of the solid line (majority) arrangement to the total one in Fig. 1, was taken into account

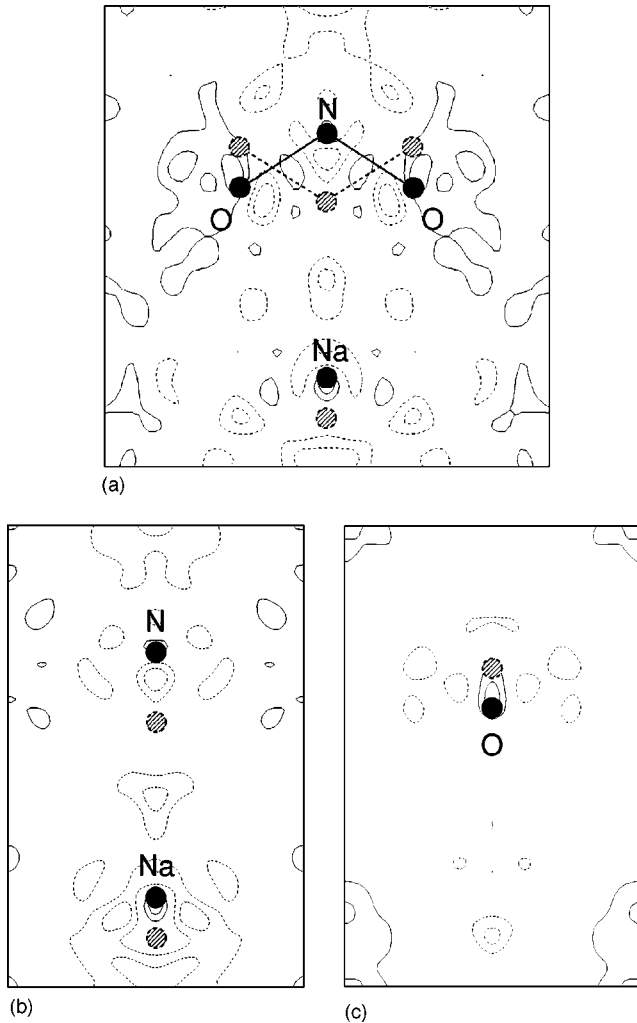


FIG. 5. Difference maps at 338 K. These maps are based on the parameters from the disordered model. In the structure factor calculations only the majority part of the model was included. (a)  $b$ - $c$  plane ( $x=1/2$ ), (b)  $a$ - $b$  plane ( $z=1/2$ ), and (c)  $a$ - $b$  plane (passing through O), respectively. Contour intervals at  $0.1 e \text{ \AA}^{-3}$ .

in the least-squares refinement (disordered model). Refinement only including the solid line arrangement (ordered model) was also performed for comparison. Refinements including the occupancy factor as adjustable parameter did not converge. So the occupancy factor was optimized step by step, with initial values estimated from the result of spontaneous polarization,<sup>29</sup> by means of seeking the values minimizing  $\chi^2$ . The order parameter  $\eta$  is represented by the occupancy factor  $\eta=2f-1$ . The refined parameters and discrepancy factors are listed in Table III. In order to reveal the evidence of the existence of a minor part arrangement, residual electron-density maps were calculated both for the disordered (Fig. 3) and for the ordered (Fig. 4) models refined against 418 K data. To show the evolution of the minority part in the disordered model with temperature, three sets of difference electron-density maps were calculated. These maps are all based on the parameters from the disordered model refined against 338 K data (Fig. 5), 378 K data (Fig. 6), and 418 K data (Fig. 7). In the structure factor

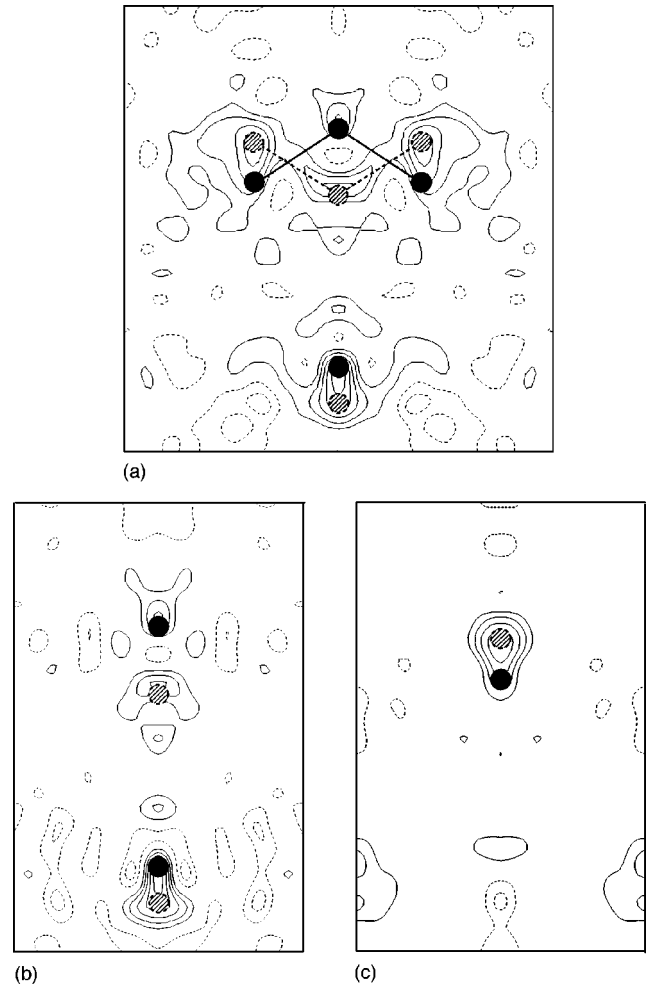


FIG. 6. Difference maps at 378 K (cf. Fig. 5). (a)  $b$ - $c$  plane ( $x=1/2$ ), (b)  $a$ - $b$  plane ( $z=1/2$ ), and (c)  $a$ - $b$  plane (passing through O), respectively. Contour intervals at  $0.1 e \text{ \AA}^{-3}$ .

calculations, only the majority part of the model was included. The maps will thus show mainly the contribution from the minority part of the electron density.

## IV. DISCUSSION

### A. Reversal of $\text{NO}_2$ ions

In the case of orthorhombic symmetry, the mean-square atomic displacements  $\langle u_i^2 \rangle$  are derived from displacement parameters  $U_{ij}$  directly,  $\langle u_i^2 \rangle = U_{ii}$ . Three simple models of  $\text{NO}_2$  reversal shown in Fig. 2 are expected to satisfy the following conditions:<sup>7</sup> (1) rotation around the  $c$  axis:  $U_{22}(N), U_{33}(N) < U_{11}(N)$  and  $U_{22}(O), U_{33}(O) < U_{11}(O)$ ; (2) rotation around the  $a$  axis:  $U_{11}(N), U_{22}(N) < U_{33}(N)$  and  $U_{11}(O), U_{33}(O) < U_{22}(O)$ ; and (3) penetration of N through two O atoms:  $U_{11}(N), U_{33}(N) < U_{22}(N)$  and  $U_{11}(O), U_{33}(O) < U_{22}(O)$ .

Our refined parameters listed in Table III show the tendency of (1) at three temperatures, which agrees with the preceding results in paraelectric phase at 448 K by Komatsu *et al.*<sup>7</sup> It is thus concluded that the relation among  $U_{ii}$  for N and O atoms is the same as in the paraelectric phase. The

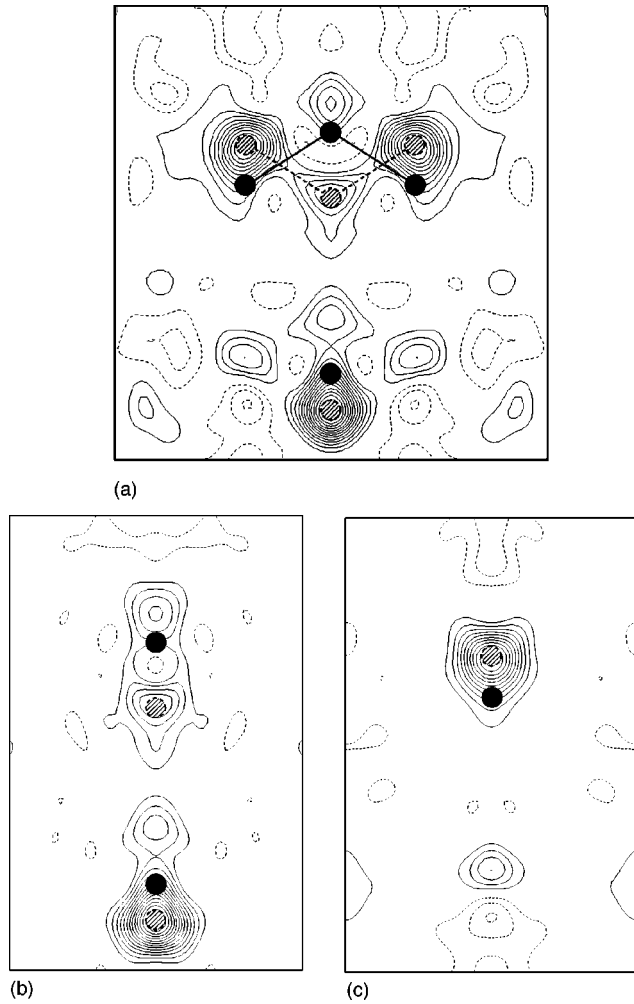


FIG. 7. Difference maps at 418 K (cf. Fig. 5). (a)  $b$ - $c$  plane ( $x=1/2$ ), (b)  $a$ - $b$  plane ( $z=1/2$ ), and (c)  $a$ - $b$  plane (passing through O), respectively. Contour intervals at  $0.1 e \text{ \AA}^{-3}$ .

difference between our results and those by Komatsu *et al.*<sup>7</sup> in the paraelectric phase is the behavior of the Na atom. In our results,  $U_{33}(\text{Na}), U_{22}(\text{Na}) < U_{11}(\text{Na})$  at each temperature while theirs are  $U_{33}(\text{Na}), U_{11}(\text{Na}) < U_{22}(\text{Na})$ .  $U_{11}(\text{Na})$  and  $U_{22}(\text{Na})$  are therefore reversed across  $T_c$ .

$U_{ii}$  for each atom are plotted in Fig. 8, together with the results of the preceding analyses in the ferroelectric phase.<sup>22-24</sup> These graphs illustrate quite clearly that the above tendency is satisfied at all temperatures and the tendency becomes stronger nearer to  $T_c$ . This fact proves that the  $\text{NO}_2$  reversal corresponds to rotation about the  $c$  axis.

### B. Rotation-translation coupling

The most interesting feature of the thermal behavior is a characteristic increase of  $U_{22}$  with temperature. The evolution of  $U_{22}$  with temperature for N and O atoms is closer to that of  $U_{33}$  than  $U_{11}$  far below  $T_c$  (quantitatively for N and qualitatively for O). However, it gets closer to that of  $U_{11}$  as temperature approaches  $T_c$ . A similar tendency can be recognized for the Na atom as well. This seems to indicate that the coupling between the translational motion along the  $b$

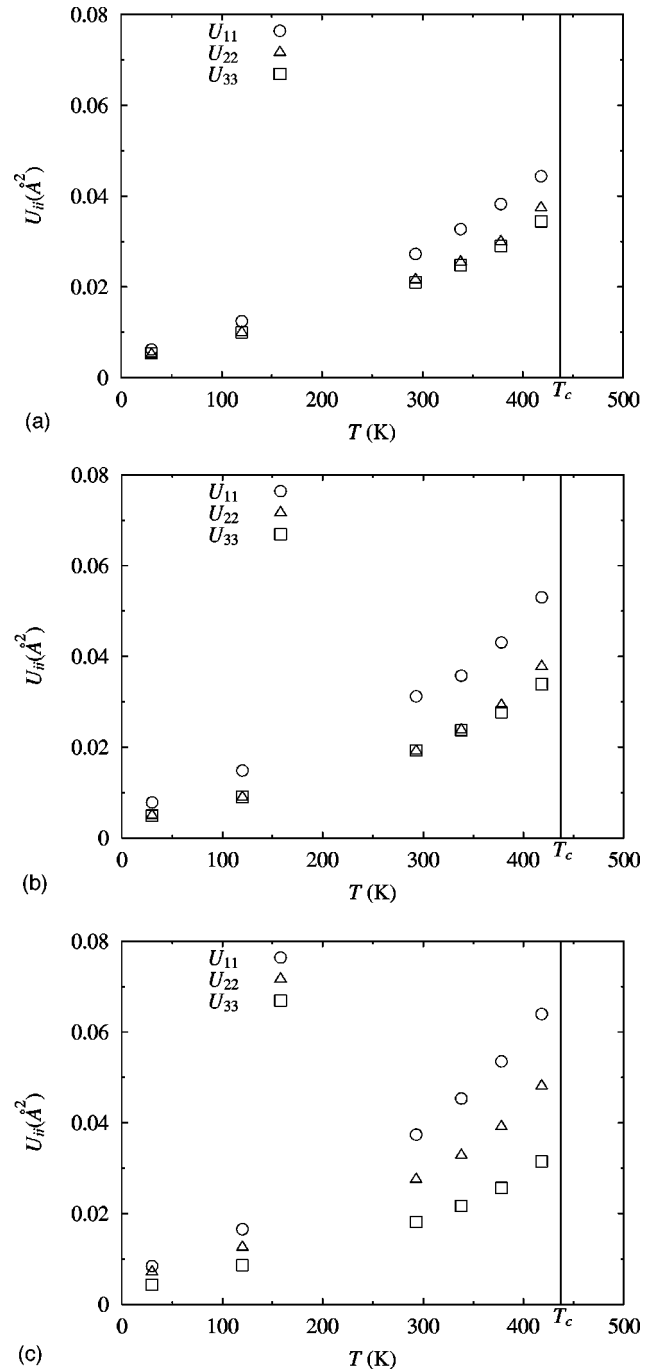


FIG. 8. Diagonal elements of the displacement parameters  $U_{ii}$  vs temperature. (a) Na, (b) N, and (c) O atom, respectively.

axis and the rotational motion around the  $c$  axis of the  $\text{NO}_2$  ion as well as the coupling between the translational motion along  $b$  and  $c$  axes of the Na ion is stronger approaching  $T_c$ . This also implies that the coupling between the thermal motions of the  $\text{NO}_2$  and Na ions is correspondingly stronger. Cooperative motion between  $\text{NO}_2$  and Na may help to reduce the effective potential barrier for  $\text{NO}_2$  rotation. This interpretation is consistent with the conclusion from microscopic models by Ehrhardt and Michel,<sup>14</sup> Kremer and Siems,<sup>16</sup> and Alfredsson.<sup>17</sup> Kremer and Siems<sup>16</sup> state that “the angular dependence of an effective local  $\text{NO}_2$ -group

potential varies strongly with restriction imposed on the coordinates of the surrounding atoms (Na ions in this case); increasing the number of relaxing variables leads, e.g., to a decrease of the flip activation energy from 0.04 eV to 0.01 eV.”

### C. Location of rotation center

The other unsolved problem is the location of the rotation center in the polarization reversal. In a model by Klein and McDonald,<sup>15</sup> the line joining the two oxygen atoms is assumed to be the rotation center. On the other hand, in a model by Ehrhardt and Michel,<sup>14</sup> the middle point between two sodium atoms in the paraelectric phase is taken as the center of rotation. The center-of-mass of the NO<sub>2</sub> ion is assumed in the model by Kremer and Siems.<sup>16</sup> The position of the rotation center in these early works thus varies considerably.

The present results offer one suggestion about the location of the center of rotation. Assuming the NO<sub>2</sub> ion as a rigid molecule, we can deduce the rotation center by dividing the spacing between N and the O-O line in the ratio of the square roots of  $U_{11}(\text{N})$  and  $U_{11}(\text{O})$ . We estimated the location of the rotation center using all the data at six temperatures. No definite temperature dependence is found. As an average of all the data we got 0.52(1), a position slightly closer to the N atom (0 at the O-O line and 1 at N).

### D. Evidence of imperfect order

Structural evidence of imperfect order in the ferroelectric phase has not been found in earlier investigations although NaNO<sub>2</sub> is considered to exhibit a typical order-disorder transition and some efforts have been made to find it.<sup>6</sup> This may be partly due to that the spontaneous polarization steeply increases below  $T_c$  and is almost completely saturated at room temperature,<sup>29,30</sup> partly due to the fact that the data with good precision are needed to reveal such a small amount of disorder.

From Figs. 5–7, we can clearly see that the electron density of the minor part of the Na and NO<sub>2</sub> ion (position of shaded circles) increases with increasing temperature. It may be noteworthy that some residual peaks are seen in the re-

sidual maps assuming complete order (Fig. 4), but on the other hand no meaningful peak can be detected in the residual density maps (Fig. 3), if the minor part of Na and NO<sub>2</sub> is also taken account in the refinement. The residual peak reported by Kay *et al.*<sup>6</sup> was not found in the present paper.

Order parameters calculated from occupancy factors were 0.984, 0.944, and 0.804 at 338, 378, and 418 K, respectively. The values of spontaneous polarization<sup>29,30</sup> estimated from the pictures in the literature give the estimated order parameters, 0.97, 0.92, and 0.80 from Ref. 29, and 0.97, 0.96, and 0.88 from Ref. 30 at 338, 378, and 418 K, respectively. Our calculated values are in good agreement with the above estimated values in both Ref. 29 and Ref. 30, except for 418 K from Ref. 30. This disagreement did not change even when we used the value at 418 K from Ref. 30 as a starting point in the refinement.

### V. SUMMARY

The displacement parameters of ferroelectric NaNO<sub>2</sub> are investigated in a wide temperature range below  $T_c$ . The order-disorder nature is also examined using the results obtained. The present paper reveals the following points:

(1) The rotation of the NO<sub>2</sub> ion around the  $c$  axis is confirmed as the mechanism of polarization reversal.

(2) It is strongly suggested that the coupling between translational motion along the  $b$  axis and rotational motion around the  $c$  axis of the NO<sub>2</sub> ion, and the coupling between translational motion along the  $b$  and  $c$  axes of the Na ion becomes stronger approaching  $T_c$ . Cooperative motion between NO<sub>2</sub> and Na may help to reduce the effective potential barrier for NO<sub>2</sub> rotation.

(3) The location of the rotation center is estimated from  $U_{33}(\text{N})$  and  $U_{33}(\text{O})$  to be 0.52, as an average of all our data, a position slightly close to the N atom.

(4) Evidence of imperfect order in the ferroelectric phase has been found.

### ACKNOWLEDGMENT

The authors thank Mr. Hilding Karlsson for collaboration in the data collection.

<sup>1</sup>M.E. Lines and A.M. Glass, *Principle and Applications of Ferroelectrics and Related Materials* (Clarendon Press, Oxford, 1977).

<sup>2</sup>Y. Sato, K. Gesi, and Y. Takagi, *J. Phys. Soc. Jpn.* **16**, 2172 (1961).

<sup>3</sup>I. Shibuya, Y. Iwata, N. Koyano, S. Fukui, S. Mitani, and M. Tokunaga, *Annu. Rep. Res. React. Inst., Kyoto Univ.* **1**, 246 (1969).

<sup>4</sup>I. Shibuya, Y. Iwata, N. Koyano, S. Fukui, S. Mitani, and M. Tokunaga, *J. Phys. Soc. Jpn.* **28**, 281 (1970).

<sup>5</sup>M.I. Kay, *Ferroelectrics* **4**, 235 (1972).

<sup>6</sup>M.I. Kay, J.A. Gonzalo, and R. Maglic, *Ferroelectrics* **9**, 179 (1975).

<sup>7</sup>K. Komatsu, K. Itoh, and E. Nakamura, *J. Phys. Soc. Jpn.* **57**, 2836 (1988).

<sup>8</sup>S. Suzuki and M. Takagi, *J. Phys. Soc. Jpn.* **30**, 188 (1971).

<sup>9</sup>N. Niimura and M. Muto, *J. Phys. Soc. Jpn.* **35**, 628 (1973).

<sup>10</sup>T. Izumi, K. Inada, H. Nakajima, and K. Kohra, *Jpn. J. Appl. Phys.* **16**, 1063 (1977).

<sup>11</sup>H. Betsuyaku, *J. Phys. Soc. Jpn.* **27**, 1485 (1969).

<sup>12</sup>S. Singh and K. Singh, *J. Phys. Soc. Jpn.* **36**, 1588 (1974).

<sup>13</sup>S.A. Ahmed and M.H. Ali, *Phys. Status Solidi B* **194**, 517 (1996).

<sup>14</sup>K.D. Ehrhardt and K.H. Michel, *Phys. Rev. Lett.* **46**, 291 (1981).

<sup>15</sup>M.L. Klein and I.R. McDonald, *Proc. R. Soc. London, Ser. A* **382**, 471 (1982).

<sup>16</sup>J.W. Kremer and R. Siems, *Ferroelectrics* **79**, 35 (1988).

- <sup>17</sup>M. Alfredsson, Ph.D. thesis, Uppsala University, 1999.
- <sup>18</sup>M.K. Barnoski and J.M. Ballantyne, *Phys. Rev.* **174**, 946 (1968).
- <sup>19</sup>E.V. Chisler and M.S. Shur *Phys. Status Solidi* **17**, 173 (1966).
- <sup>20</sup>C.M. Hartwig, E. Wiener-Avenear, and S.P.S. Proto, *Phys. Rev. B* **5**, 79 (1972).
- <sup>21</sup>Y. Iwata, N. Koyano, and I. Shibuya, *Annu. Rep. Res. React. Inst., Kyoto Univ.* **2**, 13 (1969).
- <sup>22</sup>T. Gohda, M. Ichikawa, T. Gustafsson, and I. Olovsson, *J. Korean Phys. Soc.* **32**, S189 (1998).
- <sup>23</sup>M. Okuda, S. Ohba, Y. Saito, T. Ito, and I. Shibuya, *Acta Crystallogr., Sect. B: Struct. Sci.* **46**, 343 (1990).
- <sup>24</sup>T. Gohda, M. Ichikawa, T. Gustafsson, and I. Olovsson, *J. Korean Phys. Soc.* **29**, S551 (1996).
- <sup>25</sup>F. Lissalde, S.C. Abrahams, and L. Bernstein, *J. Appl. Crystallogr.* **11**, 31 (1978).
- <sup>26</sup>L.E. McCandlish, G.H. Stout, and L.C. Andrews, *Acta Crystallogr., Sect. A: Cryst. Phys., Diffr., Theor. Gen. Crystallogr.* **31**, 245 (1975).
- <sup>27</sup>J.-O. Lundgren, *Crystallographic Programs Report UUIC-B-13-405*, Institute of Chemistry, Univ. of Uppsala, Sweden, 1983 (unpublished).
- <sup>28</sup>P.J. Becker and P. Coppens *Acta Crystallogr., Sect. A: Cryst. Phys., Diffr., Theor. Gen. Crystallogr.* **31**, 417 (1975).
- <sup>29</sup>K. Hamano *J. Phys. Soc. Jpn.* **35**, 157 (1973).
- <sup>30</sup>W. Buchheit and J. Petersson, *Solid State Commun.* **34**, 649 (1980).